

Article

Monitoring of Engineered Stones Used in Artwork Reproductions: Mechanical Characterization by Laser Vibrometry

Andres Arciniegas , Loïc Martinez , Stéphane Serfaty  and Nicolas Wilkie-Chancellor 

Laboratoire Systèmes et Applications des Technologies de l'Information et de l'Energie, UMR CNRS 8029, CY Cergy Paris Université, 5 Mail Gay Lussac, 95031 Neuville-sur-Oise, France

* Correspondence: andres.arciniegas-mosquera@cyu.fr

Abstract: Many museums have been producing reproductions for several years to replace artworks weakened by outdoor exhibition. Among these, in order to imitate the original aesthetic, the French consortium Réunion des Musées Nationaux–Grand Palais has chosen to work from large-format marble sculpture molds to complex composite materials based on resins comprising mineral fillers. However, similar to the original works of art, these reproductions age and deteriorate due to constant outdoor exposure. For this reason, current research focuses on the preventive conservation and monitoring of the structural health of these reconstructed objects. The goal of this paper was to study the resin/mineral powder composite materials used to produce cultural heritage reproductions of sculptures. This work is oriented toward a comparison of the mechanical properties of composite materials used in the replacement of cultural heritage sculptures (for instance, in the Garden of the Palace of Versailles or the Rodin Museum). The objectives were to first characterize the physical and mechanical properties of these materials in order to identify the most suitable material for cultural heritage reproduction, and secondly, to propose a method with minimal contact that obtained equivalent information as analyses performed with conventional ultrasonic techniques. These non-destructive evaluation techniques could be used for laboratory and in situ analyses. Samples of different polymer/mineral powder filler compositions were analyzed by compressional, shear and surface waves, generated by a 1 MHz center frequency ultrasonic transducer. Firstly, the measurements made it possible to evaluate the velocities of the bulk acoustic waves and extract the Young's modulus of each tested material. Secondly, in order to have minimal contact with the analyzed structure, a laser interferometry system was used to detect waves at the surface and follow their propagation. The results clearly showed the possibility of using this technique to extract mechanical characteristics of composite materials, allowing for selection of material for the reproduction of large-format statues. For different types of polymer resins, the ability of ultrasonic analysis to track the impact of rock powder (marble or slate) on the mechanical properties of these synthetic materials was clearly observed, proving that this technique holds promise for monitoring the structural health of large-format artwork.

Keywords: nondestructive techniques for cultural heritage; mechanical characterization; laser vibrometry; composite material; artwork reproduction



Citation: Arciniegas, A.; Martinez, L.; Serfaty, S.; Wilkie-Chancellor, N. Monitoring of Engineered Stones Used in Artwork Reproductions: Mechanical Characterization by Laser Vibrometry. *Appl. Sci.* **2023**, *13*, 2266. <https://doi.org/10.3390/app13042266>

Academic Editor: Antonio Di Bartolomeo

Received: 24 January 2023

Revised: 6 February 2023

Accepted: 8 February 2023

Published: 10 February 2023



Copyright: © 2023 by the authors. Licensee MDPI, Basel, Switzerland. This article is an open access article distributed under the terms and conditions of the Creative Commons Attribution (CC BY) license (<https://creativecommons.org/licenses/by/4.0/>).

1. Introduction

The Réunion des Musées Nationaux–Grand Palais, who has been producing resin reproductions of artworks, aimed to investigate the integrity of the composite materials used to replace original sculptures in historical monuments [1]. These composite materials, mostly known as artificial or engineered stones, consist of a polymer matrix (polyester or epoxy [2]) incorporating rock powder (e.g., marble or slate [3]). These kinds of materials

are experimentally well-known for their good mechanical performance and homogeneity, although few scientific studies on their characteristics have been published in the literature [4–10].

In order to address mechanical behavior issues, a complete set of properties and characterization of general materials is needed. Borsellino et al. designed an experiment using classical mechanical tests to expose the effects of both the resin and marble powder percentage on the material properties, as well as to identify a possible correlation between these factors on the performance of marble composite structures [4]. Dos Santos et al. compared three types of engineered stones against limestone and granite in their durability against temperature, assessing thermal ageing and thermal shock effects on each material's flexural strength and Young's modulus [5]. In addition, Fiore et al. demonstrated through classical mechanical characterization that plasma treatment induces improvements in all the mechanical properties of marble composite structures [7]. Moreover, in order to propose artificial marble as an alternative material in industrial settings (such as sustainable green composite materials for construction applications [9]), Ribeiro et al. studied the impact of microstructure and showed that the regular interphase resin residues improved mechanical properties [8]. Other techniques, such as Fourier transform infrared spectroscopy, scanning electron microscopy and X-ray diffraction, respectively allow us to study the chemistry of composite formation, reveal the surface features and ascertain the presence of hard phases [10].

Nevertheless, a few studies have analyzed these kinds of materials using ultrasonic methods, such as [6], who used longitudinal and shear ultrasonic wave velocities in order to calculate the values of the acoustic impedance, Poisson's ratio and elastic constants of epoxy resin/marble powder composites. Indeed, ultrasonic techniques [11] are commonly used in the nondestructive testing of materials because they can be employed both in laboratory and in situ conditions to determine and monitor physical and mechanical properties of materials such as wood [12,13], metals [14,15], polymer/composites [16–18] and rocks [19,20]. Several configurations and instrumentations have been developed for ultrasonic testing, such as contact transducers (bulk, shear and wedge), immersion techniques and laser vibrometry [11].

In the last case, scanning laser Doppler vibrometry is a widely adopted method to measure the out-of-plane vibrational displacements related to the 1D wave propagation of materials for detecting defects or estimating viscoelastic parameters [15]. Recent technological developments have led to performant 3D scanning laser Doppler vibrometers, which give access to both out-of-plane and in-plane vibrational velocity components, which combined with inverse problem approaches, allow for the identification of orthotropic elastic stiffness using 3D guided wavefield data [21]. Likewise, numerical methods, including machine-learning methods (such as clustering of multivariate data series), are also actively used in applications related to material property characterization by means of elastic guided wave propagation phenomena [22].

This study is hereby presented to estimate the mechanical properties of composite materials used in artwork reproduction by means of laser vibrometry. Different polymer/filler composite samples were studied using ultrasonic waves. Firstly, transducers in contact with the material were used to transmit and measure acoustical bulk waves in order to estimate Young's modulus (conventional ultrasonic method). Secondly, experimental surface waves were generated using a contact method [19] and spatio-temporal propagation was performed using 1D laser vibrometry [15]. The aim was to demonstrate the possibility that laser vibrometry could be used to extract equivalent mechanical information from engineered stones as obtained from using conventional ultrasonic techniques, allowing for the selection of materials. We discuss the correspondences and discrepancies of the relation between Young's modulus and surface wave velocity for the different mixtures of materials.

2. Materials and Methods

2.1. Theoretical Considerations

In cultural heritage applications, conservators and restorers refer to the properties listed in the technical sheets before choosing/purchasing materials. The Young's modulus was the only elastic property that appeared in the data sheets of the pure resins that were used in this study (described in Section 2.2.1) and from which it is possible to compare measurements. For these reasons, we chose to focus on this property.

Ultrasonic waves are propagated mechanical oscillations of discrete particles within materials [11]. The motion carried by these particles is mainly characterized by the frequency (wavelength), amplitude and velocity of the propagation of the oscillations. For solid material characterizations, ultrasonic waves are introduced to obtain the technical constants from wave velocity measurements. The relationships between mechanical parameters and ultrasonic velocities are given depending on the symmetry of the material.

Let us note that a solid is considered to be isotropic if its properties are independent of wave propagation direction. They can be characterized by two kinds of bulk waves: compressional or shear waves [11]. For homogeneous isotropic materials, Young's modulus E can be calculated from longitudinal and transverse ultrasonic waves velocities, as follows (Equation (1) [23]):

$$E = \rho v_S^2 \frac{3v_P^2 - 4v_S^2}{v_P^2 - v_S^2} \quad (1)$$

where ρ is the density, v_P is the longitudinal wave velocity and v_S is the transverse wave velocity. In semi-infinite solids, a third type of wave, called a surface (Rayleigh) wave, may arise due to the interaction of bulk waves with a free surface. The free boundary condition leads to non-dispersive wave propagation at a constant velocity. The Rayleigh wave velocity v_R is slightly less than the velocity of transverse waves v_S because the solid behaves less rigidly in the absence of material above the surface [23].

2.2. Experimental Technique

2.2.1. Materials

Two types of resins were studied, polyester and epoxy. Indeed, these selected resins are representative materials commonly used in the reproduction of statues in the garden of Versailles Castle and more broadly in the construction of composite structures needing mechanical performance, waterproofness and compatibility with fillers at a moderate cost [2]. According to the literature, pure resins and composite samples are assumed to be isotropic homogeneous materials at the investigation scale [1,2,6]. The experiments were performed on 8 parallelepipedic samples ($100 \times 100 \times 30$ mm) with and without fillers. Table 1 describes the different sample mixtures used in this study. Slate and marble are both metamorphic rocks with mechanical properties that are much higher than those of pure resins, and therefore, the fillers were assumed to be mechanically comparable materials [3].

Table 1. Materials used in the study.

Sample	Type	Proportions with Filler
OP1	Orthophtalic Polyester POLIPLAST P 374/2	<30% Slate ¹
OP2	Orthophtalic Polyester Synolite 0328-A-1	50% Marble
IP	Isophtalic Polyester CRYSTIC® GELCOAT 997SMK	50% Marble
EP	Epoxy ALCHEMIIX® EP 5241	50% Marble

¹ Exact proportions cannot be communicated due to intellectual property protection.

2.2.2. Experimental Protocol

The protocol used in this study was based on a classical study of interactions between homogeneous isotropic materials and ultrasonic waves [1,11]. For each sample, bulk waves were measured in order to calculate Young's modulus and the surface wave propagation was studied.

Bulk waves were generated using a 1 MHz broadband ultrasonic contact transducer (longitudinal or shear, 13 mm diameter, Panametrics). The bulk wave velocities were then measured in transmission mode using another similar transducer as a receiver. Rayleigh waves were generated using a 1 MHz broadband, vertically polarized shear contact transducer (13 mm diameter, Panametrics, [1,19]). In this case, the evolution of the wave over the surface was monitored using an OFV-505 vibrometer (Polytec GmbH, Waldbronn, Germany).

The ultrasonic waves were generated by applying a short electrical pulse to transmitter transducers (amplitude = 400 V, pulse width = 50 ns), controlled by the DPR300 pulser (JSR Ultrasonics/Division of Imaginant, Pittsford, NY, USA). All transmitted ultrasonic signals were recorded by a WaveSurfer 24Xs digital oscilloscope (Teledyne LeCroy, Chestnut Ridge, NY, USA). The sampling rate of each recorded signal was 100 MHz. In order to obtain a high signal-to-noise ratio, a recorded signal was obtained from an average of 1000 sweeps [1]. The setup is shown in Figure 1.

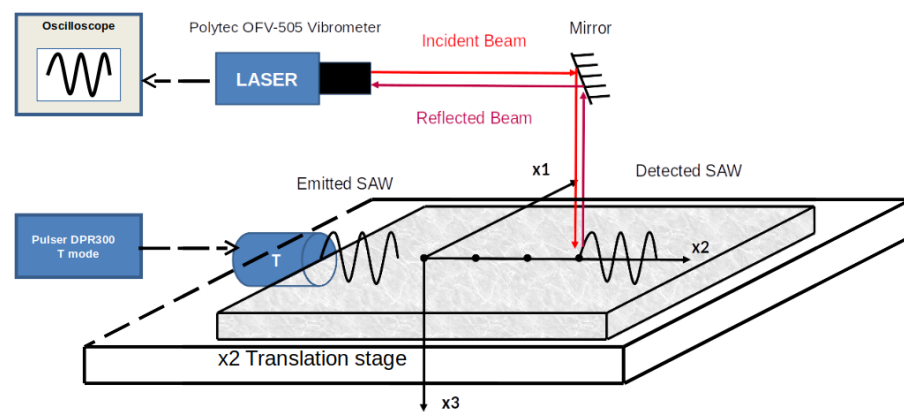


Figure 1. Rayleigh wave detection and monitoring using laser vibrometry, as performed in [1]. Firstly, a vertically polarized shear contact transducer is used to generate a surface wave. Secondly, optical detection is made by using an incident laser beam at the surface of interest and extraction of the wave signal from the Doppler shift of the reflected laser beam frequency due to the motion of the surface.

2.2.3. Bulk Wave Velocities and Young's Modulus Measurements

Considering that the material is weakly dispersive, the phase and group delays were superimposed. Longitudinal and shear wave velocities were estimated using the distance between contact transducers and the time-of-flight (TOF) of the transmitted ultrasonic pulse (Equation (2)):

$$v_{P,S} = \frac{d}{TOF} \quad (2)$$

where d is the corresponding dimension of the material in the propagating direction \vec{x}_i , such as the material length (\vec{x}_1), the material width (\vec{x}_2) or the material thickness (\vec{x}_3). Note that the P index stands for compressional wave and S stands for shear wave. In order to measure the group velocity in the three directions, TOF was determined using the max envelope method (obtained from the Hilbert transform [24]). As the material is assumed to be isotropic, $v_{P,S}$ was averaged over the three propagation directions [1]. For each sample, density was calculated from the bulk weight and volume sizing. Finally, the Young's modulus was calculated for each sample using Equation (1).

2.2.4. Rayleigh Wave Detection and Monitoring

We investigated the Rayleigh wave because the monitoring of its velocity allows us to access information from the surface of the material complementary to those given by the bulk waves. The monitoring of the Rayleigh wave was thus achieved by recording the time history received at a series of equally spaced positions along the propagation path (Figure 1 [25]). At each measurement point, the laser interferometer detected a vibration

signal at the surface. All the signals were then sorted in a spatio-temporal matrix with as many lines as measuring points. The Rayleigh wave velocity was then computed by finding the slope of the relative spatial displacement of the envelope with respect to its relative temporal displacement. Each sample was scanned over 400 measurement points along 40 mm in the x_2 axis (spatial step of 0.1 mm).

3. Results

3.1. Bulk Wave Velocities and Young's Modulus Measurements

The bulk wave velocities were measured as described in Section 2.2.3. Tables 2 and 3 show the measured values for the velocity of the longitudinal waves following the different propagating directions. For the different pure or composite samples, the maximum relative error was less than 5% (similar behavior was found for shear velocities). Taking these results into account, the isotropy and homogeneity hypothesis were verified, and from here, only average values of the longitudinal and shear wave velocities were considered for the following calculations.

Table 2. Summary of longitudinal wave velocities of the different pure samples.

Sample	v_{p1} (m·s ⁻¹)	v_{p2} (m·s ⁻¹)	v_{p3} (m·s ⁻¹)	Average v_p (m·s ⁻¹)
OP1	2255	2243	2198	2231 ± 30
OP2	2459	2458	2313	2411 ± 84
IP	2442	2396	2401	2413 ± 25
EP	2427	2342	2521	2430 ± 90

Table 3. Summary of longitudinal wave velocities of the different composite samples.

Sample	v_{p1} (m·s ⁻¹)	v_{p2} (m·s ⁻¹)	v_{p3} (m·s ⁻¹)	Average v_p (m·s ⁻¹)
OP1	2577	2566	2405	2516 ± 96
OP2	2722	2680	2479	2627 ± 130
IP	2582	2596	2417	2532 ± 100
EP	2154	2096	2195	2149 ± 41

The Young's modulus was estimated for each sample using Equation (1). Table 4 shows a comparison of the density (ρ) and Young's modulus (E) of pure and composite resins. The value of density ranged from 1021 to 1190 kg·m⁻³ and 1198 to 1702 kg·m⁻³ for pure and composite samples, respectively, confirming that composite samples are denser than pure samples. Young's modulus measurements ranged from 3.63 to 4.55 GPa for pure samples, whereas it ranged from 4.31 to 8.66 GPa for engineered stones. Hence, the values for this property were found to be higher for composite resins than pure resins.

Table 4. Summary of density (ρ) and Young's modulus (E) of the different samples.

Sample	Pure		Composite	
	ρ (kg·m ⁻³)	E (GPa)	ρ (kg·m ⁻³)	E (GPa)
OP1	1021 ± 50	3.63 ± 0.16	1251 ± 63	5.83 ± 0.89
OP2	1190 ± 68	4.55 ± 0.54	1702 ± 50	8.66 ± 1.04
IP	1097 ± 60	4.17 ± 0.26	1620 ± 99	7.43 ± 0.82
EP	1170 ± 63	3.88 ± 0.67	1198 ± 54	4.31 ± 0.46

3.2. Rayleigh Wave Detection and Monitoring

Rayleigh waves were detected using the setup described in Section 2.2.4. An example of spatio-temporal wave evolution obtained for the orthophthalic polyester composite sample OP2 is shown on Figure 2. This representation allows us to visualize the displacement of the wave envelope (light blue) in space and time (Figure 2). Thus, this spatio-temporal figure summarizes all the time signals along the 400 measurement points along the sample.

For this sample, the Rayleigh wave velocity was estimated to be about $1383 \text{ m}\cdot\text{s}^{-1}$. Table 5 shows the Rayleigh wave velocities for all the pure and composite resins. The values of this property ranged from 1075 to $1140 \text{ m}\cdot\text{s}^{-1}$ and from 1145 to $1383 \text{ m}\cdot\text{s}^{-1}$ for pure and composite samples, respectively. The maximum discrepancy in velocity was estimated to be $\pm 80 \text{ m}\cdot\text{s}^{-1}$ and was used for measurement presentation purposes.

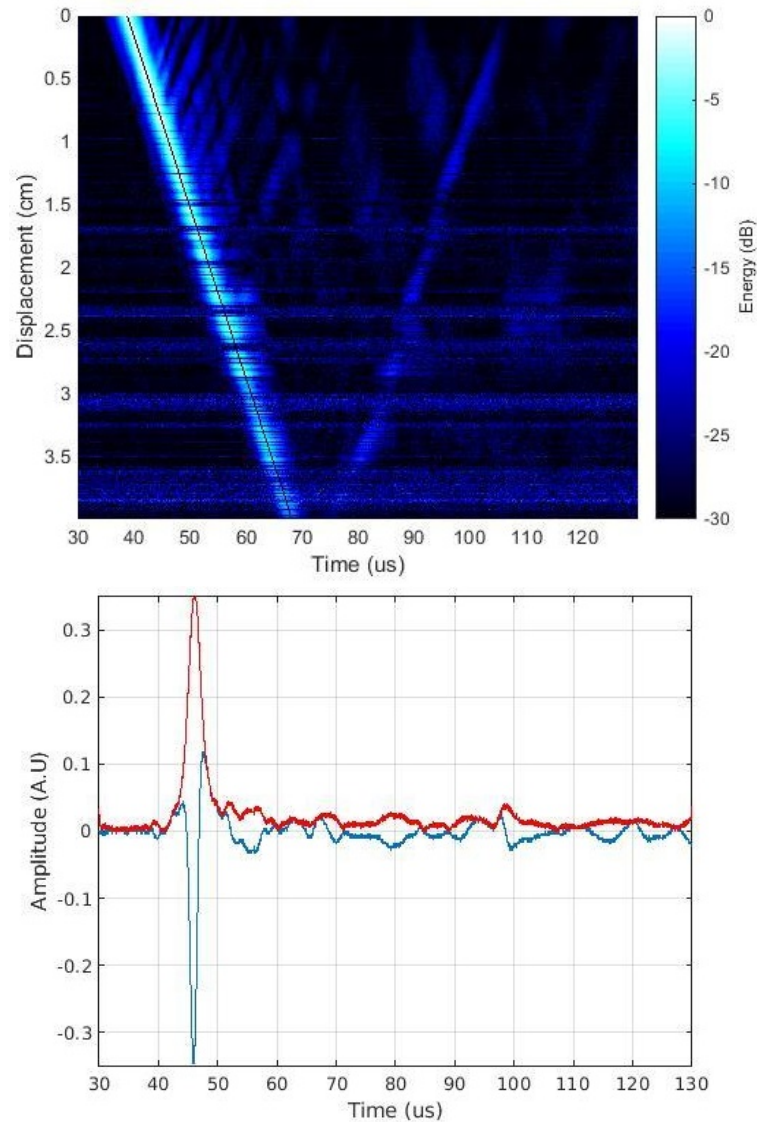


Figure 2. Spatio–temporal matrix obtained from monitoring of Rayleigh wave propagation in the OP2 sample (**above**). For $x = 1 \text{ cm}$, the signal (blue) and its envelope (red) are shown (**below**).

Table 5. Summary of Rayleigh wave velocity v_R of the different samples.

Sample	Pure	Composite
	$v_R \text{ (m}\cdot\text{s}^{-1}\text{)}$	$v_R \text{ (m}\cdot\text{s}^{-1}\text{)}$
OP1	1140 ± 80	1258 ± 80
OP2	1140 ± 80	1383 ± 80
IP	1075 ± 80	1305 ± 80
EP	1103 ± 80	1145 ± 80

4. Discussion

The practical goal of this paper was to identify the most suitable materials for cultural heritage reproduction, based on their mechanical properties measured by means

of a minimal-contact, nondestructive technique. More information is displayed by an alternative way of plotting properties [26]. Figure 3 allows us to more precisely compare the average value of the Young's modulus against the density. This chart helps with the common problem of material selection for applications in which mass must be minimized [26]. Figure 3 presents the property values for the different samples tested. One additional orthophthalic polyester/marble sample was included for comparison purposes ($\rho = 1627 \text{ kg}\cdot\text{m}^{-3}$, $E = 8.46 \text{ GPa}$, composite sample used in the garden of Versailles Castle [1]). For all samples, the results showed a directly proportional relation between both properties, confirming that the density and the Young's modulus of the resin increased for all composites as filler mass fraction increased.

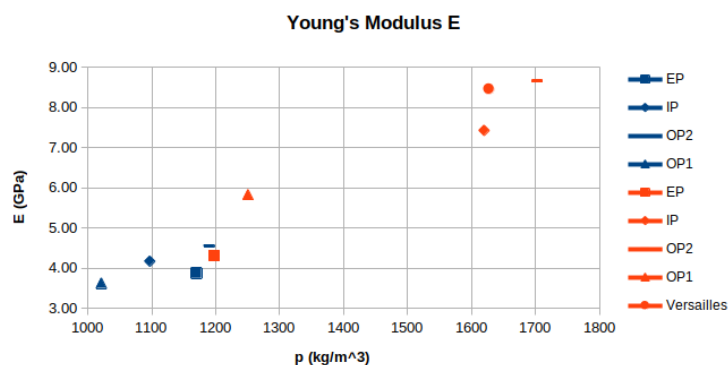


Figure 3. Young's modulus as a function of density. Pure (blue) and composite (red) resins.

In Figure 3, two groups of materials can be also distinguished: those with low and high density, correlated with low and high Young's modulus, respectively. The latter group had a remarkable Young's modulus with an average value of 8.2 GPa (average density of $1650 \text{ kg}\cdot\text{m}^{-3}$). In the case of the orthophthalic resin composite OP2, the measured properties were compatible with a Versailles reference sample [1]. This was expected as the resin type and proportions were the same for both samples. From these results, it was also observed that the isophthalic resin composite IP had comparable mechanical properties to OP2. Otherwise, the properties of the orthophthalic resin composite OP1 were closer to those of the low density group. This may have been due to the fact that the proportions of metamorphic rock filler was lower than in the case of OP2 and IP [3].

For the epoxy composite sample (EP), the obtained results were in good agreement with what is found in the literature [6], with a study measuring an average Young's modulus of 3 GPa for epoxy composites with 20% marble filler using an ultrasonic method (compared with our results, 4.31 GPa at 50% filler). However, the low Young's modulus value of EP, with respect to the other composite samples at a 50% filler mass fraction, may be due to its curing process conditions. This may lead to questions regarding the compatibility of the marble powder and epoxy, i.e., the impact of the bulk properties of the composite, for those that experienced a longitudinal velocity value decrease with respect to the pure sample.

For the different types of composites, Figures 4 and 5 make it possible to compare the average Rayleigh wave velocity against the density and Young's modulus, respectively. As previously mentioned, Figure 4 makes it possible to isolate the group of resins specific to the polyester/marble composites, such as those used in Versailles (which would be useful for identification and classification in nondestructive testing). Finally, in Figure 5, a directly proportional relationship between the Rayleigh wave velocity and the Young's modulus is observed for all the composites. In the case of polyester resins, this latter representation allows us to state that Rayleigh wave velocity and Young's modulus both increase as the filler mass fraction increases, even for the orthophthalic resin composite OP1 (whose filler mass fraction was less than 30%), which is in between the pure polyester and polyester/marble composites (50% filler). Based on the mechanical property measurements presented here, it seems more appropriate to use OP2 resins for gelcoat (pure) and imitation marble (with 50% filler) applications. Though it is not the subject of this paper, this material

is also compatible from an aesthetic point of view for the needs of restoration (visual aspect, no yellowing over time, etc.).

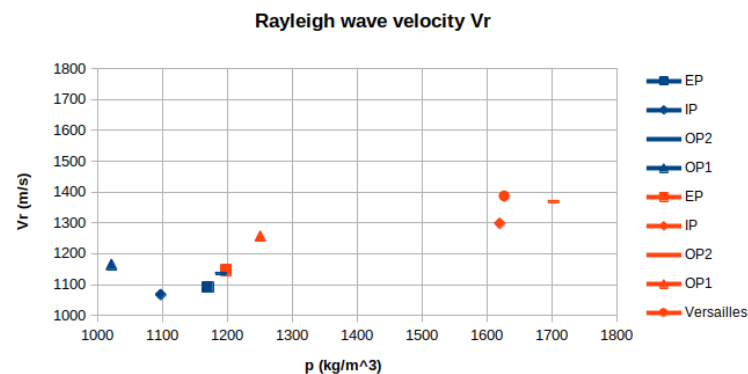


Figure 4. Rayleigh wave velocity as a function of density. Pure (blue) and composite (red) resins.

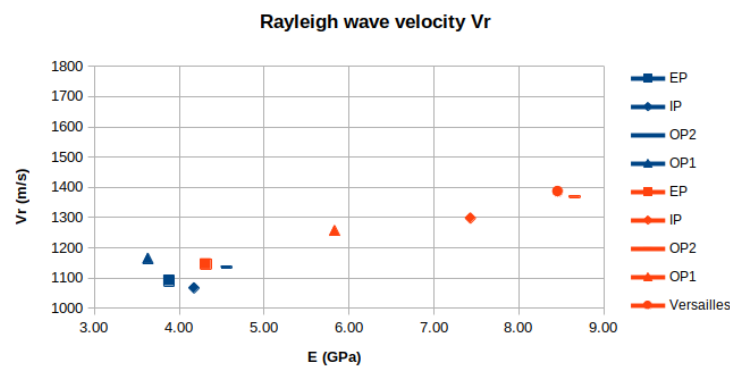


Figure 5. Rayleigh wave velocity as a function of Young's modulus. Pure (blue) and composite (red) resins.

In order to develop a nondestructive technique in cultural heritage applications, we used classical ultrasonic characterization methods. These materials were assumed to be isotropic homogeneous at the investigated scale. For the Young's modulus calculations, the measurement of ultrasonic velocities in transmission mode was used as an estimation of the average interaction of the waves through the propagation path. Calculating the wave velocity uses the apparent propagation wavepath (i.e., rectilinear) and neglects the existence of heterogeneities/defects or property gradients. It should be noted that the porosity of the composite samples was neglected because no particular distribution was found by classical mercury porosimetry. Nevertheless, porosity cannot be directly considered as an indicator explaining the variations in mechanical and acoustical properties. For the latter, the leading hypothesis is the existence of isolated pores or defects resulting from the curing process itself.

For optical measurement by vibrometry, the laser beam interacted locally with the waves propagating in the vicinity of the surface for each point of the propagation path. The measurement error was mainly due to the surface conditions, leading to low optical signal-to-noise ratio signals. As we were interested in the development of a nondestructive evaluation method based on the measurement of the Rayleigh wave, a comparison of the Rayleigh wave velocity and Young's modulus could define an experimental calibration curve of healthy samples. The accurate Young's modulus measurement based on Rayleigh wave velocity using an empirical Poisson's ratio may also be possible, as described by Li and Feng [27]. In the case of orthotropic material characterization, other techniques using full wavefield data may require the use of 3D scanning laser Doppler vibrometry and improved machine learning methods for the identification of properties such as elastic stiffness [21,22].

5. Conclusions

The aim of this research was to identify the most suitable materials in the context of cultural heritage reproduction by assessing their mechanical properties by means of a minimal-contact, nondestructive technique. This study shows the potential of using laser vibrometry to characterize engineered stones for their selection in the context of artwork reproductions. Firstly, an isotropic homogeneous hypothesis was assumed at the investigation scale in order to estimate the Young's modulus of the different composites. The error in the bulk wave velocity measurements following the different propagating directions was estimated to be less than 5%, and allowed us to verify the isotropy and homogeneity hypothesis for all the samples. Secondly, optical Rayleigh wave measurements were introduced in order to develop a minimal-contact test combining laser techniques. Comparisons were carried out to relate the Young's modulus and Rayleigh wave velocity. Our results were compared with previous studies in order to validate the method. It was shown that Rayleigh wave detection and monitoring resulted in equivalent analyses as conventional ultrasonic techniques, and may be a method to distinguish polyester composites from epoxy composites in cases of the same filler proportions. The advantage of this technique is that it allows us to access information at the surface, which is related to bulk properties. Thus, this method could be further developed using an empirical Poisson's ratio or through a statistical approach from a database including different mixture ratios. Nevertheless, there is a need to improve the theoretical modeling of these kinds of composite materials in order to define a representative testing volume, and thus overcome experimental errors induced by heterogeneities or defects that may result from their manufacturing process.

Author Contributions: Conceptualization, A.A.; Methodology, A.A.; Formal analysis, A.A.; Investigation, A.A., L.M., S.S. and N.W.-C.; Writing—original draft, A.A.; Writing—review & editing, A.A., L.M., S.S. and N.W.-C.; Supervision, N.W.-C.; Funding acquisition, S.S. All authors have read and agreed to the published version of the manuscript.

Funding: Fondation des Sciences du Patrimoine has funded this work through the project Grandes Résines.

Institutional Review Board Statement: Not applicable.

Informed Consent Statement: Not applicable.

Data Availability Statement: Not applicable.

Acknowledgments: The authors would like to thank the partners of the project for the supplied samples and Romain Martin from the LRMH for the porosity measurements of the samples.

Conflicts of Interest: The authors declare no conflict of interest.

References

1. Arciniegas, A.; Martinez, L.; Briand, A.; Prieto, S.; Serfaty, S.; Wilkie-Chancellor, N. Experimental ultrasonic characterization of polyester-based materials for cultural heritage applications. *Ultrasonics* **2017**, *81*, 127–134. [[CrossRef](#)] [[PubMed](#)]
2. Chawla, K.K. *Composite Materials*; Springer International Publishing: Cham, Switzerland, 2012. [[CrossRef](#)]
3. Mavko, G.; Mukerji, T.; Dvorkin, J. *The Rock Physics Handbook: Tools for Seismic Analysis of Porous Media*; Cambridge University Press: Cambridge, MA, USA, 2009.
4. Borsellino, C.; Calabrese, L.; Bella, G.D. Effects of powder concentration and type of resin on the performance of marble composite structures. *Constr. Build. Mater.* **2009**, *23*, 1915–1921. [[CrossRef](#)]
5. dos Santos, J.P.L.; Rosa, L.G.; Amaral, P.M. Temperature effects on mechanical behaviour of engineered stones. *Constr. Build. Mater.* **2011**, *25*, 171–174. [[CrossRef](#)]
6. Oral, I. Ultrasonic properties of epoxy resin/marble waste powder composites. *Polym. Compos.* **2015**, *36*, 584–590. [[CrossRef](#)]
7. Fiore, V.; Di Bella, G.; Scalici, T.; Valenza, A. Effect of plasma treatment on mechanical and thermal properties of marble powder/epoxy composites. *Polym. Compos.* **2016**, *39*, 309–317. [[CrossRef](#)]
8. Ribeiro, C.E.G.; Rodriguez, R.J.S.; de Carvalho, E.A. Microstructure and mechanical properties of artificial marble. *Constr. Build. Mater.* **2017**, *149*, 149–155. [[CrossRef](#)]
9. Thakur, A.K.; Pappu, A.; Thakur, V.K. Resource efficiency impact on marble waste recycling towards sustainable green construction materials. *Curr. Opin. Green Sustain. Chem.* **2018**, *13*, 91–101. [[CrossRef](#)]
10. Nayak, S.K.; Satapathy, A. Development and characterization of polymer-based composites filled with micro-sized waste marble dust. *Polym. Polym. Compos.* **2020**, *29*, 497–508. [[CrossRef](#)]

11. Krautkrämer, J. *Ultrasonic Testing of Materials*; Springer: Berlin/Heidelberg, Germany, 1990; p. 677.
12. Bucur, V.; Rocaboy, F. Surface wave propagation in wood: Prospective method for the determination of wood off-diagonal terms of stiffness matrix. *Ultrasonics* **1988**, *26*, 344–347. [[CrossRef](#)]
13. Arciniegas, A.; Prieto, F.; Brancheriau, L.; Lasaygues, P. Literature review of acoustic and ultrasonic tomography in standing trees. *Trees* **2014**, *28*, 1559–1567. [[CrossRef](#)]
14. Dayal, V. An automated simultaneous measurement of thickness and wave velocity by ultrasound. *Exp. Mech.* **1992**, *32*, 197–202. [[CrossRef](#)]
15. Wilkie-Chancellier, N.; Martinez, L.; Serfaty, S.; Griesmar, P.; Caplain, E.; Huérou, J.Y.L.; Gindre, M. Lamb mode reflections at the end of a plate loaded by a viscoelastic material. *Ultrasonics* **2006**, *44*, e863–e868. [[CrossRef](#)]
16. Hung, B.N.; Goldstein, A. Acoustic parameters of commercial plastics. *IEEE Trans. Sonics Ultrason.* **1983**, *30*, 249–254. [[CrossRef](#)]
17. Hsu, D.K.; Hughes, M.S. Simultaneous ultrasonic velocity and sample thickness measurement and application in composites. *J. Acoust. Soc. Am.* **1992**, *92*, 669–675. [[CrossRef](#)]
18. Arciniegas, A.; Achdjian, H.; Bustillo, J.; Meulen, F.V.; Fortineau, J. Experimental Simultaneous Measurement of Ultrasonic Properties and Thickness for Defect Detection in Curved Polymer Samples. *J. Nondestruct. Eval.* **2017**, *36*, 46. [[CrossRef](#)]
19. Adler, L.; Nagy, P.B. Measurements of acoustic surface waves on fluid-filled porous rocks. *J. Geophys. Res. Solid Earth* **1994**, *99*, 17863–17869. [[CrossRef](#)]
20. Bucur, V.; Rasolofoaon, P.N.J. Dynamic elastic anisotropy and nonlinearity in wood and rock. *Ultrasonics* **1998**, *36*, 813–824. [[CrossRef](#)]
21. Orta, A.H.; Kersemans, M.; Abeele, K.V.D. On the Identification of Orthotropic Elastic Stiffness Using 3D Guided Wavefield Data. *Sensors* **2022**, *22*, 5314. [[CrossRef](#)]
22. Golub, M.V.; Doroshenko, O.V.; Arsenov, M.A.; Eremin, A.A.; Gu, Y.; Bareiko, I.A. Improved Unsupervised Learning Method for Material-Properties Identification Based on Mode Separation of Ultrasonic Guided Waves. *Computation* **2022**, *10*, 93. [[CrossRef](#)]
23. Royer, D.; Valier-Brasier, T. *Elastic Waves in Solids 1*; Wiley: Hoboken, NJ, USA, 2022. [[CrossRef](#)]
24. Hughes, M.S.; Hsu, D.K. An automated algorithm for simultaneously producing velocity and thickness images. *Ultrasonics* **1994**, *32*, 31–37. [[CrossRef](#)]
25. Bouzzit, A.; Martinez, L.; Arciniegas, A.; Hebaz, S.E.; Wilkie-Chancellier, N. Rayleigh wave interaction with a spherical ball in contact with a plane surface. In Proceedings of the 2022 IEEE International Ultrasonics Symposium (IUS), Venice, Italy, 10–13 October 2022. [[CrossRef](#)]
26. Ashby, M.F. *Materials Selection in Mechanical Design*; Elsevier: Amsterdam, The Netherlands, 2005; p. 602. [[CrossRef](#)]
27. Li, M.; Feng, Z. Accurate Young’s modulus measurement based on Rayleigh wave velocity and empirical Poisson’s ratio. *Rev. Sci. Instruments* **2016**, *87*, 75111. [[CrossRef](#)] [[PubMed](#)]

Disclaimer/Publisher’s Note: The statements, opinions and data contained in all publications are solely those of the individual author(s) and contributor(s) and not of MDPI and/or the editor(s). MDPI and/or the editor(s) disclaim responsibility for any injury to people or property resulting from any ideas, methods, instructions or products referred to in the content.